

Wash-Out in N_2 -dominated leptogenesis

F. Hahn-Woernle¹

¹*Max-Planck-Institut für Physik, Föhringer Ring 6, D-80805 München, Germany*
f.hahnwo@mppmu.mpg.de

ABSTRACT: We study the wash-out of a cosmological baryon asymmetry produced via leptogenesis by subsequent interactions. Therefore we focus on a scenario in which a lepton asymmetry is established in the out-of-equilibrium decays of the next-to-lightest right-handed neutrino. We apply the full classical Boltzmann equations without the assumption of kinetic equilibrium and including all quantum statistical factors to calculate the wash-out of the lepton asymmetry by interactions of the lightest right-handed state. We include scattering processes with top quarks in our analysis. This is of particular interest since the wash-out is enhanced by scatterings and the use of mode equations with quantum statistical distribution functions. In this way we provide a restriction on the parameter space for this scenario.

Contents

1. Introduction and conventions	1
2. The orthogonal matrix and different scenarios of leptogenesis	4
3. Full Boltzmann equations for leptogenesis	7
4. Mode equations in N_2-dominated leptogenesis	10
5. Conclusions	15
A. s-channel collision integrals	16
B. t-channel collision integrals	19
C. Reaction rates in the integrated picture	21

1. Introduction and conventions

Relying on the see-saw mechanism [1–5] to create small masses for the Standard Model (SM) neutrinos, leptogenesis [6] provides an attractive explanation of the baryon asymmetry of the universe. The main ingredients of leptogenesis are the following: the out-of-equilibrium decays of the heavy right-handed neutrinos, that were added in the see-saw mechanism, into leptons and Higgs particles violate CP , from which a lepton asymmetry can be generated. This lepton asymmetry is then partially transformed into a baryon asymmetry by anomalous processes of the SM called sphalerons [7]. In this way the three Sakharov conditions are fulfilled and leptogenesis turns out as a consequence of the see-saw mechanism.

In the minimal (type-I) see-saw model, gauge singlet fermions with Majorana masses M_i , eigenvalues of the complex symmetric 3×3 Majorana mass matrix M_M , couple to the massless lepton doublet and to the Higgs doublet of the SM through Yukawa couplings given by the 3×3 matrix λ_ν . These Yukawa couplings then generate a Dirac mass term $m_D = \lambda v$, where $v = 174 \text{ GeV}$ is the vacuum expectation value of the Higgs field, relating the heavy singlets to SM neutrinos upon spontaneous symmetry breaking of the electroweak gauge symmetry. In the see-saw mechanism the eigenvalues of the Majorana mass matrix are much larger than the Dirac mass matrix entries, $M_{M_i} \gg m_{D_i}$, and the mass matrix of the left-handed states is then suppressed by the high-energy scale M ,

$$m_{\nu_{ij}} = -v^2 \lambda_{ik} M_{M_k}^{-1} \lambda_{kj}. \quad (1.1)$$

Participating in Yukawa couplings, the heavy neutrinos are unstable and the total decay width of a right-handed neutrino generation N_i at tree-level is given by

$$\Gamma_{D_i} = \sum_{\alpha} (\Gamma_{i\alpha}(N_i \rightarrow \Phi + l_{\alpha}) + \bar{\Gamma}_{i\alpha}(N_i \rightarrow \bar{\Phi} + \bar{l}_{\alpha})) = \frac{1}{8\pi} (\lambda^{\dagger} \lambda)_{ii} M_i, \quad (1.2)$$

where the sum is taken over the single decay rates into lepton flavor α . The CP asymmetry in lepton flavor α is then defined as

$$\varepsilon_{i\alpha} \equiv \frac{\Gamma_{i\alpha}(N_i \rightarrow \Phi + l_{\alpha}) - \bar{\Gamma}_{i\alpha}(N_i \rightarrow \bar{\Phi} + \bar{l}_{\alpha})}{\sum_{\alpha} (\Gamma_{i\alpha}(N_i \rightarrow \Phi + l_{\alpha}) + \bar{\Gamma}_{i\alpha}(N_i \rightarrow \bar{\Phi} + \bar{l}_{\alpha}))}, \quad (1.3)$$

This asymmetry is due to the interference of the tree-level amplitude and the one-loop vertex and self-energy contributions. The indices i and α denote the generation of the decaying right-handed neutrino and the flavor of the produced lepton, respectively. Accounting for different lepton generations, the CP asymmetry is a diagonal matrix in flavor space. It has been shown in [8–12] that the flavor structure of the final state leptons has sizable implications on leptogenesis predictions. To account for the lepton flavor structure one introduces the projectors

$$P_{i\alpha} \equiv |\langle l_i | l_{\alpha} \rangle|^2 = P_{i\alpha}^0 + \frac{\Delta P_{i\alpha}^0}{2}, \quad (1.4)$$

$$\bar{P}_{i\alpha} \equiv |\langle \bar{l}'_i | \bar{l}_{\alpha} \rangle|^2 = P_{i\alpha}^0 - \frac{\Delta P_{i\alpha}^0}{2}. \quad (1.5)$$

The wash-out rate in inverse decays is then reduced by the projector $P_{i\alpha}^0 = (P_{i\alpha} + \bar{P}_{i\alpha})/2$, since the Higgs will make inverse decays on flavor eigenstates $|l_{\alpha}\rangle$ instead of the linear superposition $|l_i\rangle$. The second effect, an additional CP -violating contribution, stemming from a different flavor composition between $|l_i\rangle$ and $CP|\bar{l}'_i\rangle$, can be expressed by the projector difference $\Delta P_{i\alpha} = P_{i\alpha} - \bar{P}_{i\alpha}$. The sum over flavor of this difference results in $\sum_{\alpha} \Delta P_{i\alpha}^0 = 0$. The decay rates into single lepton flavor α are now given by $\Gamma_{i\alpha} \equiv P_{i\alpha} \Gamma_i$ and $\bar{\Gamma}_{i\alpha} \equiv \bar{P}_{i\alpha} \bar{\Gamma}_i$, and the flavored CP asymmetries can be written in terms of the unflavored asymmetries

$$\varepsilon_{i\alpha} = P_{i\alpha}^0 \varepsilon_i + \frac{\Delta P_{i\alpha}^0}{2}. \quad (1.6)$$

The second term gives the contribution due to a potentially different flavor composition between $|l_i\rangle$ and $|\bar{l}'_i\rangle$. Summing these CP asymmetries over the flavor yields the total CP asymmetry used in the unflavored regime $\varepsilon_i = \sum_{\alpha} \varepsilon_{i\alpha}$. In this paper we will mainly be interested in the effects of a full spectral distribution of right-handed neutrinos on leptogenesis and not in the effects of the lepton flavor structure. Therefore we will perform all calculations in the so-called alignment case, that is realized when the N_i -decays are just into one flavor α , resulting in $P_{i\alpha} = \bar{P}_{i\alpha} = 1$, $P_{i\beta \neq \alpha} = \bar{P}_{i\beta \neq \alpha} = 0$ and $\varepsilon_{i\alpha} = \varepsilon_i$. In this case the kinetic equations, c.f. Section 3, are identical to the kinetic equations used in the unflavored regime that is realized at $T \gtrsim 10^{12}$ GeV. By restricting to the alignment case we can compare our results to the ones obtained in previous calculations using unflavored Boltzmann equations [21–23]. However, we will keep all flavor indices in our notation, since all results are valid when considering independently the single flavors α . We will comment on the effects of the lepton flavor structure in more detail later in Section 2.

Summing over all lepton flavors, $\varepsilon_i = \sum_{\alpha} \varepsilon_{i\alpha}$, the CP asymmetry can be written as [13–15]

$$\varepsilon_i \approx -\frac{1}{8\pi} \sum_{\substack{j=1,2,3 \\ j \neq i}} \frac{\text{Im} \left[(\lambda^\dagger \lambda)_{ij}^2 \right]}{(\lambda^\dagger \lambda)_{ii}} \times \left[f_V \left(\frac{M_j^2}{M_i^2} \right) + f_S \left(\frac{M_j^2}{M_i^2} \right) \right], \quad (1.7)$$

where the vertex (f_V) and the self-energy (f_S) contributions are

$$f_V(x) = \sqrt{x} \left[1 - (1+x) \log \left(\frac{1+x}{x} \right) \right], \quad \text{and} \quad f_S(x) = \frac{\sqrt{x}}{1-x}. \quad (1.8)$$

The out-of-equilibrium dynamic that is necessary for successful leptogenesis is provided by the expansion of the universe. One usually compares the total decay rate of the right-handed neutrino state given in Eq. (1.2) to the expansion rate at temperatures $T \sim M_i$,

$$H(T = M_i) = \sqrt{4\pi^3 g^*/45} (M_i/M_{\text{Pl}}), \quad (1.9)$$

introducing the decay parameters

$$K_i \equiv \frac{\Gamma_{D_i}}{H(M_i)} = \frac{\tilde{m}_i}{m_*}, \quad (1.10)$$

where $M_{\text{Pl}} = 1.221 \times 10^{19}$ GeV is the Planck mass, and $g^* = 106.75$ corresponds to the number of relativistic degrees of freedom in the SM at temperatures higher than the electroweak scale. One introduces at this point two dimensionful variables to connect the decay parameters to the neutrino mass scale via the *effective neutrino mass* [16] \tilde{m}_i and the *equilibrium neutrino mass* m_* :

$$\tilde{m}_i = \frac{v^2 (\lambda^\dagger \lambda)_{ii}}{M_i}, \quad \text{and} \quad m_* = \frac{16\pi^{\frac{5}{2}} \sqrt{g^*}}{3\sqrt{5}} \frac{v^2}{M_{\text{Pl}}} \approx 1.08 \times 10^{-3} \text{ eV}. \quad (1.11)$$

The decay parameters for each flavor α are again given via the projectors

$$K_{i\alpha} \equiv P_{i\alpha}^0 K_i. \quad (1.12)$$

The decay parameters control whether the right-handed neutrino decays in equilibrium ($K_{i\alpha} > 1$) or out of equilibrium ($K_{i\alpha} < 1$) and are key quantities for the dynamics of leptogenesis.

In general, the baryon asymmetry produced by leptogenesis can be written as [17]

$$\eta_B = \frac{3}{4} \frac{\alpha_{\text{sph}}}{f} \sum_{i,\alpha} \varepsilon_{i\alpha} \kappa_{i\alpha}^f \equiv d \sum_{i,\alpha} \varepsilon_{i\alpha} \kappa_{i\alpha}^f \simeq 0.96 \times 10^{-2} \sum_i \varepsilon_i \kappa_i^f, \quad (1.13)$$

where in the last step the sum over the flavor α has been performed as it is possible in the alignment case or in the unflavored regime at $T \gtrsim 10^{12}$ GeV. The final efficiency factors κ_i^f , that parametrize the amount of asymmetry that survives the competing production and wash-out processes are direct results of solving the relevant Boltzmann equations for leptogenesis [18, 19]. In the limit of vanishing wash-out and a thermal initial abundance for the right-handed neutrinos, the efficiency factors have a final value $\kappa_i^f = 1$. The factor $f = 2387/86$ accounts for the dilution of the baryon asymmetry due to photon production from the onset of leptogenesis till recombination and the quantity

$\alpha_{\text{sph}} = 28/79$ is the conversion factor of the $B - L$ asymmetry into a baryon asymmetry by the sphaleron processes.

The most simple realization of thermal leptogenesis is the N_1 -dominated scenario, where a lepton asymmetry is exclusively generated in the decays of the lightest right-handed state N_1 . Qualitatively, this scenario can be realized assuming $M_1 \ll M_2 \ll 10^{14} \text{ GeV} \ll M_3$. Then the heaviest right-handed state N_3 decouples [20] and this typically implies a hierarchy in the CP asymmetries, i.e., $|\varepsilon_3| \ll |\varepsilon_2| \ll |\varepsilon_1|$, as a consequence of light particles in the internal lines of the self-energy and vertex corrections to the tree-level decay diagram. Indeed, in the limit of massless particles in the internal lines, the corresponding CP asymmetry vanishes, cf. Eq. (1.7). Furthermore, due to N_1 interactions following the decays of the heavier right-handed states $N_{2,3}$, a substantial part of the produced lepton asymmetry will presumably be washed-out, especially in the regime of strong wash-out.

In this paper we will go beyond the simplest scenarios and consider leptogenesis in a set-up where the asymmetry is generated in the decays of the next-to-lightest state N_2 , that is called the N_2 -dominated scenario [21]. The viability of N_2 -dominated leptogenesis is restricted by the wash-out of produced asymmetry induced by interactions of the lightest state N_1 that tend to destroy any previously created lepton asymmetry. We will address this issue of wash-out in N_2 -dominated leptogenesis within the simple alignment case, that is equivalent to the unflavored regime, by means of complete Boltzmann equations at the mode level including scattering with top quarks [22] and extend on the previous studies of [23] where only decays and inverse decays were considered. We show how the additional wash-out due to quantum statistical distribution functions and scattering processes restricts the valid parameter space of N_2 -dominated leptogenesis.

In the next section we show how specific scenarios of leptogenesis can be realized by specifying the relevant see-saw parameters and discuss qualitatively the N_1 - and N_2 -dominated scenarios. In Section 3 we present Boltzmann equations for leptogenesis including scattering at the mode level and apply these equations to study N_2 -dominated leptogenesis quantitatively in Section 4. In the Appendices A, B, and C we list explicitly the integral expressions used to solve the Boltzmann equations.

2. The orthogonal matrix and different scenarios of leptogenesis

To understand how specific scenarios of leptogenesis can be realized, we recast the light neutrino mass matrix, Eq. (1.1),

$$m_\nu = -m_D \frac{1}{M_M} m_D^T,$$

with $m_D = \lambda v$. Here, it is always possible to choose a basis in which the heavy neutrino mass matrix is diagonal, $D_M = \text{diag}(M_1, M_2, M_3)$. Using an unitary matrix U , one can simultaneously diagonalize the light neutrino mass matrix

$$D_m = -U^\dagger m_\nu U^*, \quad (2.1)$$

where $D_m = \text{diag}(m_1, m_2, m_3)$. If one does not account for the running of neutrino parameters from the electroweak scale to the see-saw scale [24, 25], the matrix U corresponds to the

Pontecorvo–Maki–Nakagawa–Sakata (PMNS) matrix. In the basis where the charged leptons mass matrix is diagonal and with the help of an orthogonal matrix Ω , the Dirac neutrino mass matrix can be written in the so-called *Casas–Ibarra parametrization* [26],

$$m_D = U \sqrt{D_m} \Omega \sqrt{D_M}. \quad (2.2)$$

The Dirac neutrino mass matrix is fully described by 18 parameters: the mixing matrix U contains six parameters (three mixing angles and three phases), the diagonal matrices D_m and D_M contain three neutrino masses each, and the orthogonal matrix Ω is described by six real (three complex) parameters. It can be written as a product of three rotational matrices [21, 27]

$$\Omega(\omega_{21}, \omega_{31}, \omega_{32}) = R_{12}(\omega_{21}) R_{13}(\omega_{31}) R_{23}(\omega_{32}), \quad (2.3)$$

with

$$R_{12} \equiv \begin{pmatrix} \pm\sqrt{1-\omega_{21}^2} & -\omega_{21} & 0 \\ \omega_{21} & \pm\sqrt{1-\omega_{21}^2} & 0 \\ 0 & 0 & \pm 1 \end{pmatrix}, \quad (2.4)$$

$$R_{13} \equiv \begin{pmatrix} \pm\sqrt{1-\omega_{31}^2} & 0 & -\omega_{31} \\ 0 & \pm 1 & 0 \\ \omega_{31} & 0 & \pm\sqrt{1-\omega_{31}^2} \end{pmatrix}, \quad (2.5)$$

and

$$R_{23} \equiv \begin{pmatrix} \pm 1 & 0 & 0 \\ 0 & \pm\sqrt{1-\omega_{32}^2} & -\omega_{32} \\ 0 & \omega_{32} & \pm\sqrt{1-\omega_{32}^2} \end{pmatrix}. \quad (2.6)$$

In general, one can state that Eq. (2.2) is divided into two parts: (i) a measurable low-energy part, containing the PMNS matrix U and the light neutrino masses D_m , and (ii) a high-scale part, consisting of the orthogonal Ω matrix and the heavy neutrino masses D_M , which is not accessible by current experiments.

The N_1 -dominated scenario can now be realized assuming the heavy neutrino mass matrix to be hierarchical, i.e. $M_1 \ll M_2 \ll M_3$, together with a specific choice of the CP asymmetries implemented by a special form of the Ω matrix [21, 27]:

- For $\Omega = R_{13}$, the CP asymmetry in N_2 decays vanishes, i.e., $\varepsilon_2 = 0$, while ε_1 is maximal.
- For $\Omega = R_{12}$, the CP asymmetry ε_1 is suppressed compared to its maximal value, and $|\varepsilon_2| \propto (M_1/M_2) |\varepsilon_1|$ is negligible within a strong mass hierarchy¹.

In [17, 28, 29] it has been shown that the N_1 -dominated scenario proves to be independent of the initial conditions in the regime of strong wash-out. However, in the weak wash-out regime the final

¹If $M_1 \sim M_2$, both CP asymmetries should be taken into account.

asymmetry production depends sensibly on the initial conditions of the N_1 abundance. Furthermore, thermal leptogenesis sets a lower limit of $M_1 \gtrsim 10^9$ GeV [30] on the mass of the lightest right-handed neutrino in order to explain successfully the observed value of the baryon asymmetry of the universe. This bound is consequently translated into a lower bound on the reheating temperature after inflation, $T_{RH} \gtrsim 1.5 \times 10^9$ GeV [31]. These lower bounds not only have an issue with the cosmological abundance of gravitinos [32–35] within supersymmetric theories, but also cause some specific problems in grand unified theories based on flavor models. Some of these models assume a grand unified symmetry between up-quarks and neutrinos. The neutrino Yukawa couplings are then connected with the up-quark Yukawa matrices leading to right-handed neutrino masses that are proportional to the square of the up-quark masses [36, 37]. Typical values for the mass of the lightest right-handed state fall in the range $10^6 - 10^7$ GeV, see e.g., [38, 39], and masses $M_1 \geq 10^9$ GeV need a specific choice of parameters [40, 41]. This makes thermal leptogenesis difficult to reconcile with this class of models.

In order to circumvent these issues, the N_2 -dominated scenario was proposed in [21]. Indeed, for $\Omega = R_{23}$ one can have a maximal CP asymmetry ε_2 coming from N_2 decays while ε_1 vanishes. This means that N_1 is totally decoupled from the heavier states while in the N_2 decays the heavy third state, N_3 , runs in the internal lines of the one-loop diagrams. Together with a mass hierarchy in the heavy neutrinos, N_2 -dominated leptogenesis can be realized if the wash-out from N_1 interactions does not deplete the produced asymmetry. With the above choice of Ω , the effective neutrino mass of the lightest right-handed state is fixed to $\tilde{m}_1 = m_1$. Thus, for hierarchical light neutrino masses the N_1 interactions can be forced to be in the weak wash-out regime where $\tilde{m}_1 \lesssim m^* \approx 10^{-3}$ eV. It is worth noticing that, if the N_1 interactions are in the weak wash-out regime, i.e., $\tilde{m}_1 < m^*$, then the N_2 interactions are constrained to be in the strong wash-out regime, i.e., $\tilde{m}_2 > m^*$. This is due to the orthogonality of the Ω matrix [21]. Therefore, N_2 -dominated leptogenesis is independent of the initial conditions on N_2 . In order to achieve a large enough CP asymmetry, the lower bound on the mass M_1 can be directly translated into a bound on the mass M_2 , whereas the lower bound on the reheating temperature remains unchanged. The lower bound on M_1 is then evaded and M_1 can be arbitrarily light compatibly with the see-saw condition $M \gg m_D$. However, allowing for small complex rotations R_{12} and R_{13} , both of these bounds become increasingly more stringent leading to a point beyond which the N_2 -dominated scenario is not viable anymore.

Note on flavor

Considering flavor effects beyond the alignment case may substantially change the parameter ranges in which the scenarios discussed above are valid. When the flavor structure of the lepton asymmetry and the wash-out is tracked, it is possible to generate a large enough lepton asymmetry in N_2 decays even if N_1 interactions are effective. It has been shown in [41] that the N_1 -induced wash-out of an asymmetry, established in the lepton state l_2 via N_2 decays², can be sizably effected by the projector $P_{1\alpha} = |\langle l_1 | l_\alpha \rangle|^2$ that leads to a reduction of the wash-out strength, i.e., $K_{1\alpha} < K_1$. Another possible modification is that the coherence of the lepton state l_2 is destroyed by potentially fast occurring N_1 inverse decays. This leads to a statistically mixed state consisting

²The states $|l_i\rangle = 1/\sqrt{(\lambda^\dagger \lambda)_{ii}} \sum_\alpha \lambda_{\alpha i} |l_\alpha\rangle$ are participating in interactions with the heavy states N_i [45].

Table 1: Scenarios in the decays/inverse decays pictures (D1 and D4) and scenarios including scattering with the top quark (S1 and S2) and their associated assumptions. Cases D1 and S1 correspond to the conventional integrated Boltzmann approach, while Cases D4 and S2 involve solving the full set of Boltzmann equations at the mode level. The naming of the different scenarios corresponds to [22].

Case	kinetic equilibrium	quantum statistics
D1	Yes	No
D4	No	Yes
S1	Yes	No
S2	No	Yes

of l_1 and the state orthogonal to l_1 . As a result, parts of the asymmetry, stored in the state orthogonal to l_1 , are protected from N_1 wash-out [42–44]. This is only possible when the N_1 states decay in the two-flavor regime at temperatures $10^9 \text{ GeV} \lesssim T \lesssim 10^{12} \text{ GeV}$, where only the τ Yukawa interactions are in equilibrium, or in the unflavored regime at temperatures $T \gtrsim 10^{12} \text{ GeV}$. In the fully flavored regime, however, the full flavor basis is resolved and there does not exist any direction in flavor space that is protected against N_1 wash-out [45]. The study of [46] considered the case $\Omega = R_{12}(\omega_{21}) R_{13}(\omega_{31})$ together with $\omega_{32} = 0$ for values $M_1 \gtrsim 10^9 \text{ GeV}$, lying in the two-flavor regime. It was found that even for small values $\omega_{21} \leq 0.1$ the contribution to the asymmetry from N_2 decays can be naturally the dominant one for $10^{11} \text{ GeV} \lesssim M_2 \lesssim 10^{14} \text{ GeV}$, when the effects of flavor on the N_1 -induced wash-out are taken into account.

Furthermore, in Section 1 we did not account for the effect of flavor on the CP asymmetry. In Eq. (1.3) we wrote the CP asymmetry as a matrix in flavor space. Indeed, the hierarchy of CP asymmetries, following a mass hierarchy of particles in the internal lines, does not necessarily hold when flavored asymmetries are considered [11]. In contrast to the unflavored scenario, where ε_2 is suppressed by M_1/M_2 compared to ε_1 when assuming $M_1 \ll M_2 \ll 10^{14} \text{ GeV} \ll M_3$, there is the possibility of having a non-negligible asymmetry $\varepsilon_{2\alpha}$ that, in turn, eventually extends the range of the N_2 -dominated scenario.

3. Full Boltzmann equations for leptogenesis

In this paper we study the wash-out of a lepton asymmetry by means of the full Boltzmann equations at the mode level including scattering with the top quark in the alignment case where $K_{i\alpha} = K_i$ and $K_{i\alpha\neq\beta} = 0$. This study does not rely on the assumption of kinetic equilibrium for right-handed neutrinos and will not restrict the distribution functions to be classical. In order to study the effects of quantum statistical distribution functions and scattering with top quarks we specify different scenarios shown in Table 1. The mode equations including scattering processes based on the Yukawa coupling with the top quark for right-handed neutrinos and the lepton asym-

metry are given by

$$\frac{H(M_i)}{z_i} \frac{\partial f_{N_i}}{\partial z_i} = C_D [f_{N_i}] + 2 C_{S,s} [f_{N_i}] + 4 C_{S,t} [f_{N_i}], \quad (3.1)$$

$$\frac{H(M_i)}{z_i} \frac{\partial f_{(l-\bar{l})_\alpha}}{\partial z_i} = C_D [f_{(l-\bar{l})_\alpha}] + 2 C_{S,s} [f_{(l-\bar{l})_\alpha}] + 4 C_{S,t} [f_{(l-\bar{l})_\alpha}], \quad (3.2)$$

where $z_i = M_i/T$. The right-hand sides of Eqs. (3.1) and (3.2) contain one collision integral from decays/inverse decays and two collision integrals from scattering processes coming, respectively, from scattering in the s -channel and in the t -channel at tree level. Here, one factor of 2 stems from contributions from processes involving anti-particles, and another factor of 2 in the t -channel terms originates from the u -channel diagram.

In our analysis we only include tree-level scattering processes that are of $\mathcal{O}(h_t^2 \lambda^2)$ [22]. We do not consider interactions with gauge bosons, nor include CP violation in $2 \rightarrow 2$ or $1(2) \rightarrow 3$ processes, which are of higher order in the Yukawa couplings. The effect of CP violation from these processes was considered in [9, 47–49]. The numerical integration of Eqs. (3.1) and (3.2) over the right-handed neutrino (lepton) phase space results in the time evolutions of the number densities n_{N_i} and $n_{(l-\bar{l})_\alpha}$. Normalization to the equilibrium photon number density $n_\gamma^{\text{eq}} = (\zeta(3)/\pi^2) g_\gamma T^3$, with $g_\gamma = 2$, gives the comoving abundances N_{N_i} ($N_{(l-\bar{l})_\alpha}$). The decay collision integrals for the right-handed neutrinos and the lepton asymmetry can be evaluated analytically to be [23, 50]

$$C_D [f_{N_i}] = \frac{\Gamma_{D_i} z_i}{\mathcal{E}_N y_N} f_{N_i}^{\text{eq}} (-1 + f_{N_i} + e^{\mathcal{E}_N} f_{N_i}) \log \left[\frac{\sinh((\mathcal{E}_N - y_N)/2)}{\sinh((\mathcal{E}_N + y_N)/2)} \right], \quad (3.3)$$

$$C_D [f_{(l-\bar{l})_\alpha}] = -\frac{\Gamma_{D_{i\alpha}} z_i}{2y_l^2} \int_{\frac{z_i^2 - 4y_l^2}{4y_l}}^{\infty} dy_N \frac{y_N}{\mathcal{E}_N} \left[(f_\Phi + f_{N_i})(f_{(l-\bar{l})_\alpha} + \varepsilon_{i\alpha} F_\alpha^+) - 2\varepsilon_{i\alpha} f_{N_i} (1 + f_\Phi) \right] + \mathcal{O} \left(\lambda_{\alpha i}^2 \lambda_{\beta i}^2 \times f_{(l-\bar{l})_\beta} \right), \quad (3.4)$$

where $F_\alpha^+ = f_{l_\alpha} + f_{\bar{l}_\alpha}$, $\mathcal{E}_j = E_j/T$, $y_j = |\mathbf{p}_j|/T$,³ and f_Φ denotes the distribution function of the Higgs particle. Up to subleading corrections, that are of higher order in the Yukawa couplings, the collision integrals in the different flavors decouple and the corresponding Boltzmann equations can be solved in analogy to the single flavor case.⁴ For SM particles we assume Fermi–Dirac distributions for leptons and a Bose–Einstein distribution for the Higgs particle, since gauge interactions lead to very fast equilibration rates [51].

The scattering collision integrals are nine-dimensional and cannot be evaluated analytically. However, they can be reduced analytically to two-dimensional integrals given by [22]

$$C_{S,(s,t)} [f_{N_i}] = \sum_\mu \frac{3T}{2^6 \pi^3 \mathcal{E}_N y_N} \frac{h_t^2(T) M_i \tilde{m}_1}{v^2} \quad (3.5)$$

$$\times \int_{w(\mathcal{E}_N, l, q, t)}^{u(\mathcal{E}_N, l, q, t)} d\mathcal{E}_l \int_{l(\mathcal{E}_N, l, q, t)}^{k(\mathcal{E}_N, l, t, q)} d\mathcal{E}_{(t,q)} \Lambda_{(s,t)}^{(N)} I_{(s,t)}^{(\mu)}, \quad (3.6)$$

³For better clearness we drop the generation index for the heavy neutrinos in \mathcal{E}_N and y_N and the flavor index for the leptons in y_l .

⁴Reference [23] includes terms in addition to Eq. (3.4) in order to avoid asymmetry production in thermal equilibrium. However, the same analysis also shows that the quantitative difference between this and our approach is negligible.

for the right-handed neutrino and

$$C_{S,(s,t)} \left[f_{(l-\bar{l})_\alpha} \right] = \sum_{\mu} \frac{3T}{2^6 \pi^3 \mathcal{E}_l^2} \frac{h_t^2(T) M_i \tilde{m}_1}{v^2} \times \int_{w(\mathcal{E}_{N,l,q,t})}^{u(\mathcal{E}_{N,l,q,t})} d\mathcal{E}_N \int_{l(\mathcal{E}_{N,l,q,t})}^{k(\mathcal{E}_{N,l,q,t})} d\mathcal{E}_{(t,q)} \Lambda_{(s,t)}^{(l-\bar{l})_\alpha} I_{(s,t)}^{(\mu)}, \quad (3.7)$$

for the asymmetry. Here, $h_t^2(T)$ is the top Yukawa coupling evaluated at the leptogenesis scale z_i and the functions $\Lambda_{(s,t)}^N$ and $\Lambda_{(s,t)}^{(l-\bar{l})_\alpha}$ denote the phase space factors for the right-handed neutrino (lepton) scatterings in the s - and t -channel, respectively. The integration limits u , w , k , and l depend on the energies of the particles involved in the interactions and give the distinct integration ranges for each integrand in the sums of Eqs. (3.5) and (3.7). The integrands consist of the phase space factors and the analytical functions $I_{(s,t)}^\mu$, that encode the matrix element and the result of the angle integration. Both depend on the energies of the particles involved in the process. For the s -channel diagram the sum contains six terms for the right-handed neutrino and the lepton asymmetry and for the t -channel diagram one counts four terms each. The explicit expressions of the single collision integrals are listed in the Appendices A and B and the rather lengthy derivation can be found in the appendices of [22, 52].

Inserting Eqs. (3.5) and (3.7) in the Boltzmann equations (3.1) and (3.2) yields the complete set of differential equations to be integrated numerically. Once the Boltzmann equations for the distribution functions are solved, one can perform the integration over the right-handed neutrino (lepton) phase space to obtain the number densities and, in turn, the efficiency factors

$$\kappa_{i\alpha} = \frac{4}{3} \frac{\varepsilon_{i\alpha}^{-1}}{\alpha_{\text{sph}} - 1} N_{(l-\bar{l})_\alpha}. \quad (3.8)$$

A value of $\sum_{\alpha} N_{(l-\bar{l})_\alpha} = 3.14 \times 10^{-8}$ is needed in order to explain the value $\eta_B^{\text{CMB}} = (6.225 \pm 0.17) \times 10^{-10}$, measured in Cosmic Microwave Background (CMB) observations by the WMAP satellite [53].

With the restriction on classical equilibrium distribution functions of the Maxwell–Boltzmann type and assuming kinetic equilibrium holds for the heavy right-handed neutrinos, Eqs. (3.1) and (3.2) can be integrated over the right-handed neutrino (lepton) phase space to recast the Boltzmann equations in an integrated form [17],

$$\frac{dN_{N_i}}{dz} = - (D_i + S_i) \left(N_{N_i} - N_{N_i}^{\text{eq}} \right), \quad (3.9)$$

$$\frac{dN_{(l-\bar{l})_\alpha}}{dz} = -W_{i\alpha} N_{(l-\bar{l})_\alpha} + \varepsilon_{i\alpha} D_i \left(N_{N_i} - N_{N_i}^{\text{eq}} \right), \quad (3.10)$$

where $N_j = n_j/n_\gamma^{\text{eq}}$. The quantities D_i (S_i) account for the production of right-handed neutrinos from inverse decays (scatterings), and the wash-out rate $W_{i\alpha}$ contains as well contributions from both, scatterings (W_α^S) and inverse decays $W_{i\alpha}^{ID} = P_{i\alpha}^0 W_i^{ID}$. The explicit expressions for D_i , S_i , $W_{i\alpha}$, and $N_{N_i}^{\text{eq}}$ can be found in Appendix C.

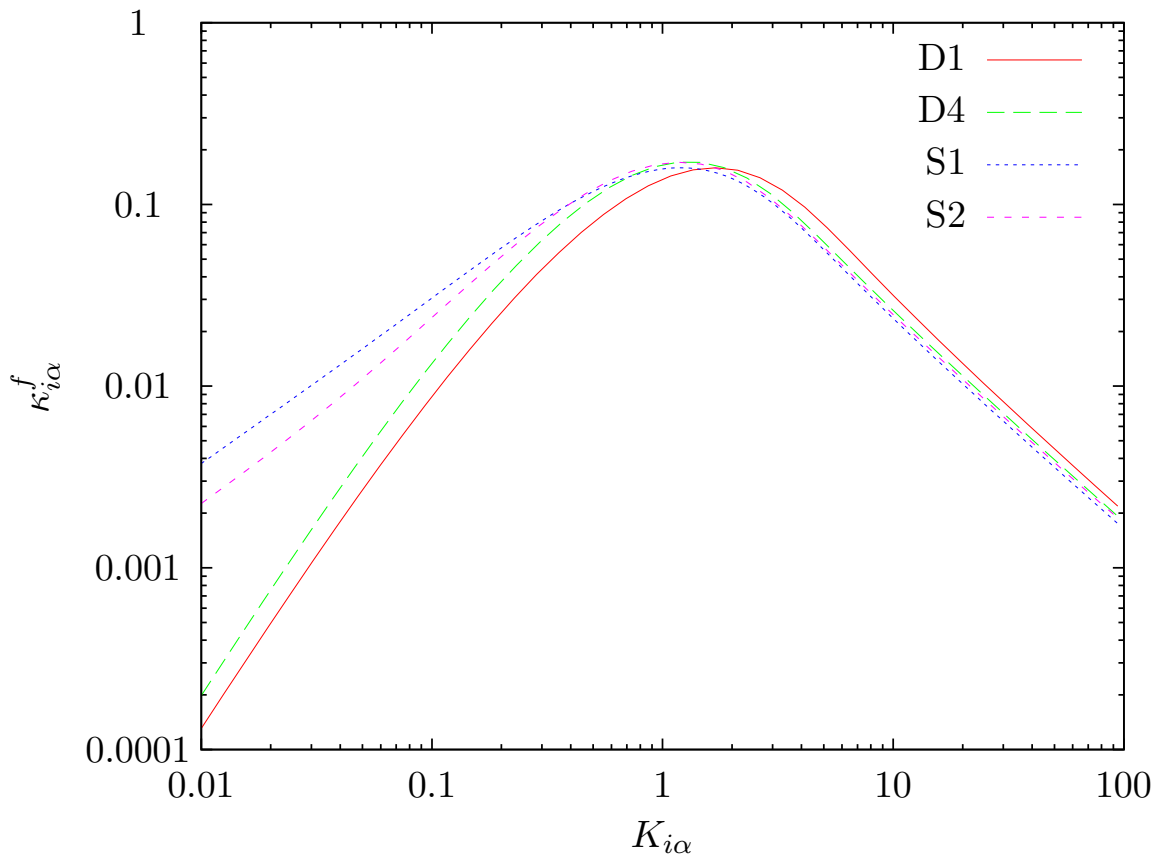


Figure 1: The final efficiency factors $\kappa_{i\alpha}^f$ at the production stage for a vanishing initial N_i abundance in dependence of the interaction parameter $K_{i\alpha}$. Shown are the two cases including scattering processes S1 (dotted/blue) and S2 (short dashed/magenta), and two scenarios D1 (solid/red) and D4 (long dashed/green) within the decay–inverse decay only framework [22].

4. Mode equations in N_2 -dominated leptogenesis

The general effects of the full spectral distributions of right handed neutrinos on the production of a lepton asymmetry in thermal leptogenesis have been discussed extensively in [22], where the final efficiency factors for the scenarios, presented in Table 1, have been calculated. The results can be summarized in Figure 1, where the final efficiency factors as a function of $K_{i\alpha}$ are shown for the integrated approach (Cases D1 and S1) and the complete mode treatment (Cases D4 and S2), both including and excluding scattering. For Cases S1 and S2 which include scattering, we note that their difference is rather large in the weak wash-out regime ($K_{i\alpha} < 1$), with the integrated approach overestimating $\kappa_{i\alpha}^f$ by up to a factor ~ 1.5 at $K_{i\alpha} \sim 0.01$ compared to solving the complete mode equations. But this difference decreases as we increase $K_{i\alpha}$. At $K_{i\alpha} \gtrsim 3$ the integrated approach underestimates $\kappa_{i\alpha}^f$ by less than $\sim 10\%$. It is also interesting to note that the relative contribution of scattering processes to the final efficiency factor is smaller in the complete mode calculation than in the integrated approach. In the weak wash-out regime, including scattering enhances the final efficiency factor from decays and inverse decays by up to a factor of ~ 30 in the integrated scenario. In the complete mode calculation, however, the enhancement is only a factor of ~ 15 .

Similarly, in the strong wash-out regime, scattering reduces $\kappa_{i\alpha}^f$ by up to 20% in the integrated picture, compared to below 10% in the complete treatment.

In this section, however, we want to discuss the effects the complete set of mode equations, cf. Eqs. (3.1) and (3.2), have in the N_2 -dominated scenario.

Here, the wash-out due to N_1 interactions is (i) enhanced using mode-equations with decays/inverse decays alone and (ii) enhanced including scatterings with the top quark. We will not

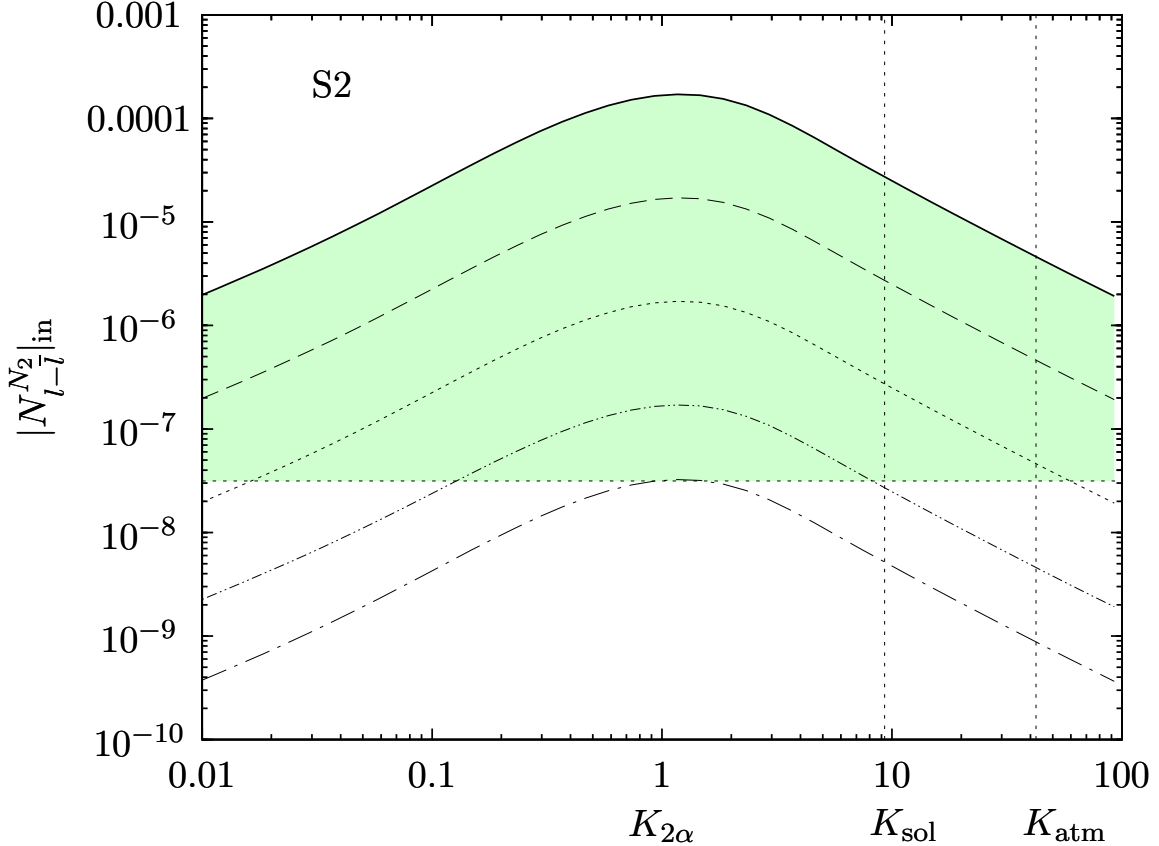


Figure 2: Lepton asymmetry generated in N_2 decays for $\varepsilon_{2\alpha} = 10^{-6} (M_2/10^{10} \text{ GeV})$ and different values of M_2 in the Case S2 for a vanishing initial N_2 abundance: (i) $M_2 = 10^{13} \text{ GeV}$, solid line, (ii) $M_2 = 10^{12} \text{ GeV}$, long-dashed line, (iii) $M_2 = 10^{11} \text{ GeV}$, dashed line, (iv) $M_2 = 10^{10} \text{ GeV}$, point-point-dashed line, and (v) $M_2 = 1.9 \times 10^9 \text{ GeV}$, point-dashed line. Within the considered scenario, the shaded region indicates where the produced baryon asymmetry exceeds η_B^{CMB} . The allowed values of $|N_{l-\bar{l}}^{N_2}|_{\text{in}}$ will be taken as initial values to calculate the wash-out induced by N_1 -interactions. The differences induced when considering the Cases D1, D4 and S1 can directly be read-off from Figure 1.

study N_2 -dominated leptogenesis with a specific form for the Ω matrix but rather consider values of $K_{1\alpha}$ and $K_{2\alpha}$ going from the weak wash-out regime ($K_{i\alpha} = 0.01$) up to the strong wash-out regime ($K_{i\alpha} = 100$) without the restrictions that are usually imposed when choosing a specific Ω matrix constellation. For example one usually has $K_{2\alpha} \gtrsim K_{\text{sol}} \sim 9$ for Ω_{23} [21, 46]. In doing so we can study the effect of the enhanced wash-out due to scattering and the use of mode equations on the N_1 -induced wash-out and restrict the general available parameter space for N_2 -dominated leptogenesis in terms of $M_{1,2}$ and $K_{(1,2)\alpha}$. A similar study has been performed in [23] where,

however, wash-out effects have been considered in the decay-inverse decay only picture.

The lepton asymmetry that can be generated in N_2 decays is shown in Figure 2 in dependence of the decay parameter $K_{2\alpha}$ for values of M_2 varying between 1.9×10^9 GeV and 10^{13} GeV. The shaded area marks the region where the final asymmetry exceeds the value η_B^{CMB} , measured in the observation of the Cosmic Microwave Background. For $M_2 \lesssim 2 \times 10^9$ GeV the CP asymmetry generated in N_2 decays is too small to account for the observed value of the matter–antimatter asymmetry.⁵ We assumed the maximal value of the CP asymmetry $\varepsilon_{2\alpha}^{\text{max}} \approx 10^{-6} (M_2/10^{10} \text{ GeV})$ to be realized. In specific scenarios, however, the CP asymmetry $\varepsilon_{2\alpha}$ will be smaller and the corresponding lower bound will be at $M_2 \gtrsim 10^{10}$ GeV [21]. On the other hand, for $M_2 \gtrsim 10^{13}$ GeV one has to account for $\Delta L = 2$ violating scattering processes with the N_2 in the s - and t -channel. Being an additional contribution to the wash-out, these processes tend to reduce the final amount of asymmetry [54]. The two vertical lines in Figure 2 correspond to the solar and atmospheric neutrino scales, respectively. Considering the N_2 interactions to be in the strong wash-out regime in the window preferred by neutrino oscillation data demands $M_2 \gtrsim 10^{11}$ GeV to explain the observed value of the baryon asymmetry.

The lepton asymmetry generated in N_2 decays is altered by the subsequent wash-out due to interactions of the lightest right-handed neutrino N_1 . According to the considerations of [23], where N_2 -dominated leptogenesis has been addressed by means of mode equations within the decay–inverse decay only scenario (Case D4), we choose the following initial conditions at $z_1 = M_1/T$ to calculate the effect of wash-out on an initially produced asymmetry: (i) We take $|N_{l-\bar{l}}^{N_2}|_{\text{in}} = 10^{-7}$ as initial value of the lepton asymmetry generated in N_2 decays, (ii) assume a zero initial N_1 abundance, and (iii) set $\varepsilon_{1\alpha} \approx 0$. The third condition can be achieved by supposing a small value of the N_1 mass. Anyway, small lepton asymmetries stemming from different generations add up linearly and an additional asymmetry $\varepsilon_{1\alpha}$ would not modify our considerations on the N_1 -induced wash-out effects. We choose $M_1 = 10^7$ GeV in the numerical implementation in order to fix the evolution of the top Yukawa coupling.

Figure 3 shows on the left panel the time evolution of the normalized N_1 number density for the Cases D1, D4, S1, and S2 in dependence of z_1 and $M_1 = 10^7$ GeV. On the right panel the time evolution of the lepton asymmetry during N_1 wash-out is shown for the same scenarios. Thus, in addition to the discussion in [23], we include Cases S1 and S2 here. In the weak wash-out regime ($K_{1\alpha} = 0.1$), the asymmetry is only slightly reduced in the Cases D4, S1, and S2 compared to the integrated approach in the decay-inverse decay only scenario, Case D1. The net wash-out of the initial asymmetry is less than 10%. However, already at $K_{1\alpha} \sim 1$ the strength of the wash-out in the different scenarios becomes distinguishable. At $z_1 \sim 1$ wash-out becomes effective and is strongest in Case S2 where the complete set of Boltzmann equations including scattering with the top quark is considered. However, the net reduction of the initial asymmetry is still less than one order of magnitude. The difference in the lepton asymmetry between Case D4 and Case S2, both using mode equations, is very small (below 2 %) and cannot be seen in Figure 3.⁶ Comparing Case S2 with Case S1, we see that the influence of the additional wash-out factor f_{N_1} , present in the mode equation, cf. Eq. (3.4), is larger than the wash-out due to scatterings in the integrated approach that

⁵This bound on M_2 is more severe than the value given in Section 2 since for a vanishing initial abundance $\kappa_{i\alpha}^f < 1$.

⁶An error in the numerical calculation for the Case D4, appearing in an earlier publication [52], that leads to larger differences between the Cases D4 and S2, has been corrected in the present paper.

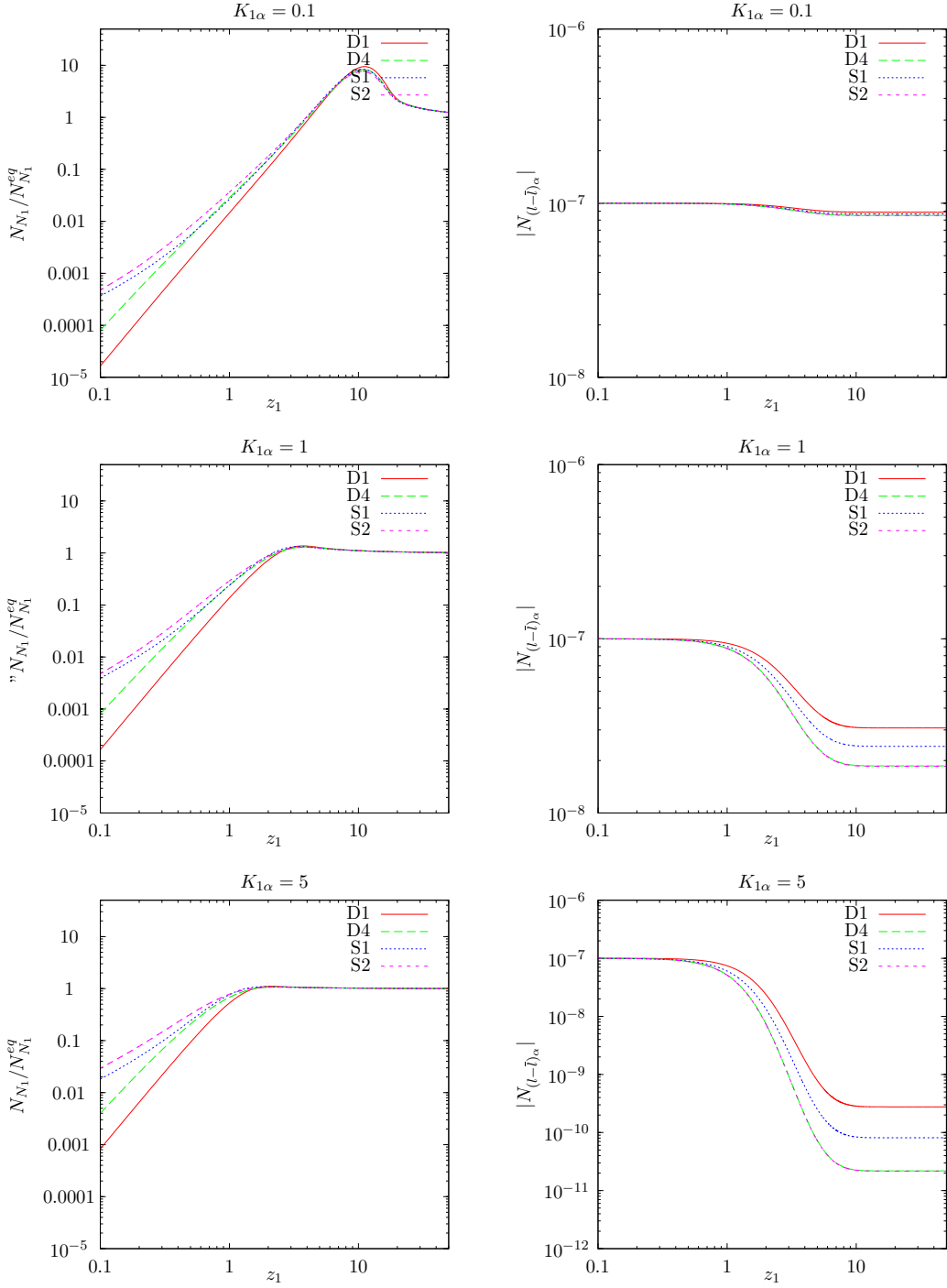


Figure 3: Time evolution of the absolute value of the normalized right-handed neutrino number density $N_{N_1}/N_{N_1}^{eq}$ and the lepton asymmetry $|N_{(l-\bar{l})_\alpha}|$ for three different coupling strengths $K_{1\alpha}$ in the N_2 -dominated scenario for an initial asymmetry $|N_{l-\bar{l}}^{N_2}|_{in} = 10^{-7}$, $M_1 = 10^7$ GeV and a vanishing initial N_1 abundance. The differences between the Cases D4 and S2 are smaller than 2 %.

is present in Case S1. In the strong wash-out regime, for $K_{1\alpha} = 5$, the initial asymmetry is depleted by up to two orders of magnitude, with the strongest wash-out again in Case S2. Considering the

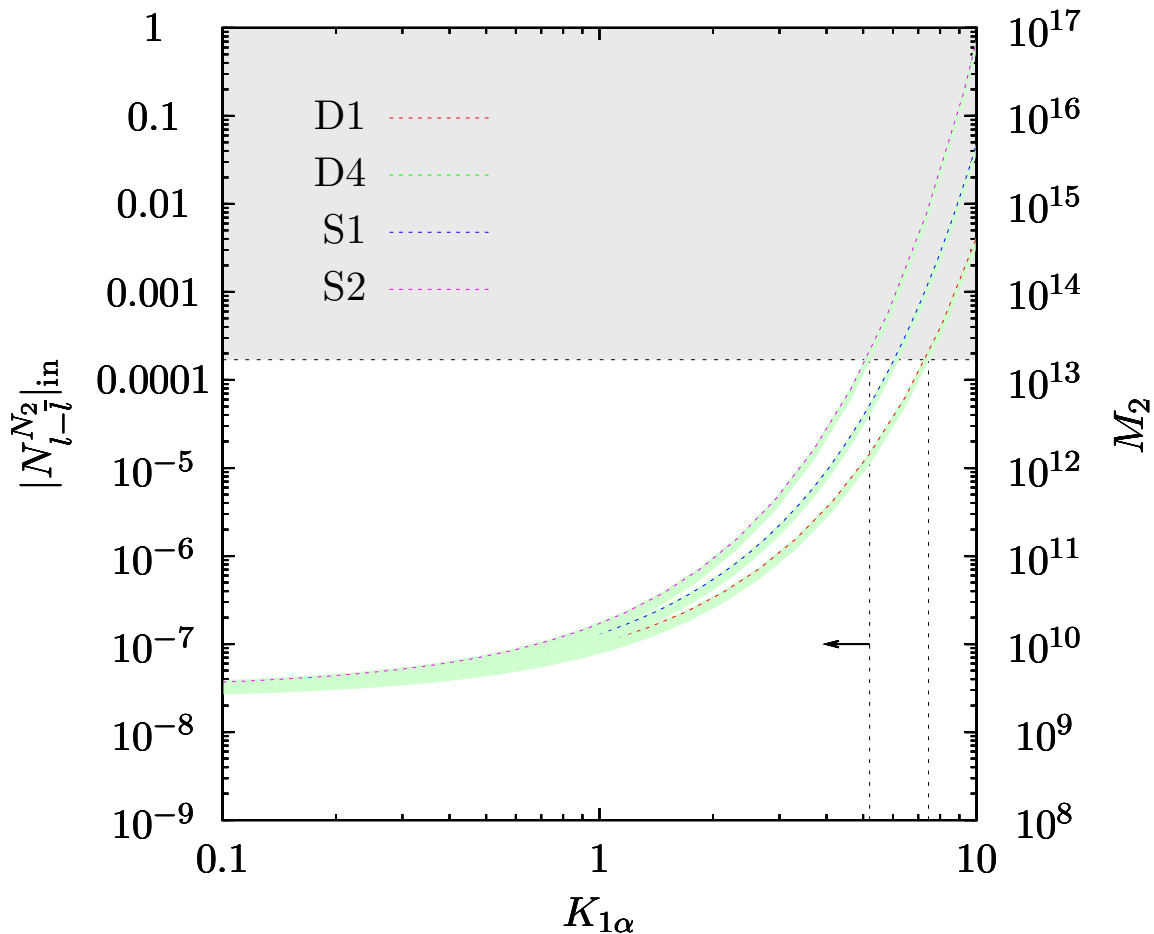


Figure 4: Amount of initial asymmetry that has to be generated in N_2 decays in order to survive the subsequent wash-out by N_1 interactions for the Cases D1, D4, S1 and S2. The mass of the lightest right-handed neutrino was set to $M_1 = 10^7$ GeV and the CP asymmetry generated in N_1 decays was set $\varepsilon_{1\alpha} = 0$. The mass M_2^{S2} , that is needed to produce enough initial asymmetry in N_2 decays when $K_{2\alpha} \approx 1$, is shown on the right vertical axis for the Case S2. The asymmetry in the gray shaded region cannot be generated in N_2 decays and the area right of the arrow is excluded due to N_1 wash-out.

momentum integrated scenarios, the reduction in Case S1 is two orders of magnitude larger than in Case D1. Concerning the scenarios in which mode equations are used, the contribution of the scatterings amounts again less than 2 % as can be seen by comparing Case S2 with Case D4. In general, it can be stated that the wash-out is enhanced more by the use of mode equations (due to an additional wash-out factor f_{N_1}) than by the inclusion of scattering processes that become important only for values $K_{1\alpha} \geq 1$ in the integrated approach (Case S1).

Figure 4 shows the amount of initial asymmetry generated in N_2 decays that is needed to account for the observed value of the baryon asymmetry after wash-out due to N_1 interactions in dependence of $K_{1\alpha}$ for the Cases D1, D4, S1 and S2. For the Case S2, the mass of the next-to-lightest neutrino M_2^{S2} , that is needed to produce enough initial asymmetry when $K_{2\alpha} \approx 1$, is shown on the right vertical axis. The green colored regions correspond to the value of the baryon asymmetry deduced in Big Bang Nucleosynthesis (BBN) within 95% confidence level [55], and the

dashed-lines within this regions represent the value of the baryon asymmetry deduced from CMB measurements. When N_1 interactions fall into the weak-wash-out regime ($K_{1\alpha} < 1$), almost all of the initial generated asymmetry survives giving $|N_{l-\bar{l}}^{N_2}|_{\text{in}} \approx 3 \times 10^{-8}$, i.e., the same limit as can be seen in Figure 2 and the different Cases D1, D4, S1 and S2 cannot be distinguished. However, increasing the strength of the N_1 interactions, wash-out becomes more and more effective and for $K_{1\alpha} \gtrsim 1$ the differences between the Cases D1, D4 and S2 become visible. Again, considering the treatment with mode equations (Cases D4 and S2), the contributions of the scatterings are below 2 % and too small to be visible in Figure 4. For $K_{1\alpha} = 10$ an initial value $|N_{l-\bar{l}}^{N_2}|_{\text{in}} \approx 1$ is needed to account for the observed value of the baryon asymmetry. Though, as can be seen in Figure 2, values of the asymmetry lying in the shaded area above the horizontal dashed line at $|N_{l-\bar{l}}^{N_2}|_{\text{in}} = 1.7 \times 10^{-4}$ cannot be generated in N_2 decays. Therefore, for the N_2 -dominated scenario to be successful, the N_1 interactions are restricted to $K_{1\alpha} \lesssim 5$ for the Cases S2 and D4. When considering the integrated Case D1, this bound can be relaxed to $K_{1\alpha} \lesssim 7$. Considering Case S2, the upper bound on the initial asymmetry corresponds to values $M_2^{S2} = 10^{13}$ GeV and $K_{2\alpha} \approx 1$ as can be seen on the right vertical axis of Figure 4. For values of $K_{2\alpha}$ lying in the strong wash-out regime, that is preferred by neutrino oscillation data, the generated asymmetry is roughly one order of magnitude smaller, leading to $K_{1\alpha} \lesssim 3$ in Case S2 and $K_{1\alpha} \lesssim 4$ for Case D1. When choosing conservative values, $M_2 \approx 10^{11}$ GeV and $\kappa_{2\alpha}^f \approx 10^{-2}$, the scenarios are forced to $K_{1\alpha} \lesssim 2$ for Case S2 and $K_{1\alpha} \lesssim 3$ for D1.⁷ This corresponds to values of $K_{1\alpha}$ typically needed in $SO(10)$ inspired GUTs where flavor effects are included. For the limiting scenario, $M_2 \approx 2 \times 10^9$ GeV, the N_1 interactions strength $K_{1\alpha}$ has to vanish [56] in all considered cases.

5. Conclusions

In this paper we studied leptogenesis in an alternative scenario where the lepton asymmetry is created in the decays of the next-to-lightest right-handed neutrino state N_2 . Here, the additional wash-out present in the complete set of mode equations leads to a more efficient depletion of the lepton asymmetry in interactions of the lightest right-handed neutrino N_1 ; these interactions follow the asymmetry generation in the decays of the heavier state. In order to account for the observed value of the matter-antimatter asymmetry, the possible values of the decay parameters $K_{1\alpha}$ and $K_{2\alpha}$ of the two right-handed states can be restricted. From the maximal amount of asymmetry that is achievable in N_2 decays, the decay parameter of the lightest right-handed neutrino is forced to $K_{1\alpha} \lesssim 5$ when accounting for the spectral distribution of right-handed neutrinos. The effects of scattering process on the N_1 -induced wash-out are smaller than 2 %. Furthermore, demanding the decay parameter $K_{2\alpha}$ to be in the strong wash-out regime favored by neutrino oscillation data, where the asymmetry generation is independent of the initial conditions on N_2 , sets the more stringent limit $K_{1\alpha} \lesssim 2$.

Note added

After the present paper was submitted, a new analysis of leptogenesis in the N_2 -dominated scenario appeared [58], in which the effects of flavor on the CP asymmetries in N_2 -dominated leptogenesis are studied in detail.

⁷Using typical assumptions, the study in [23] found a limit $K_{1\alpha} < 3$.

Acknowledgments

We thank Steve Blanchet and Michael Plümacher for useful discussions and comments.

Appendices

A. s -channel collision integrals

Right-handed neutrino

Using energy conservation, and Fermi–Dirac statistics for the leptons and quarks, the phase space factor reads

$$\Lambda_s^{(N_i)}(f_{N_i}, f_{l_\alpha}, f_t, f_q) = - \frac{e^{\mathcal{E}_l + \mathcal{E}_t} (-1 + f_{N_i} + e^{\mathcal{E}_N} f_{N_i})}{(1 + e^{\mathcal{E}_l}) (1 + e^{\mathcal{E}_t}) (e^{\mathcal{E}_l + \mathcal{E}_N} + e^{\mathcal{E}_t})}. \quad (\text{A.1})$$

The s -channel contribution to Eq. (3.5) is then given by,

$$C_{S,s}[f_{N_i}] = C_s^{(1)} + C_s^{(2)} + C_s^{(3)} + C_s^{(4)} + C_s^{(5)} + C_s^{(6)}, \quad (\text{A.2})$$

The single collision integrals must be evaluated numerically and then summed to give $C_{S,s}[f_{N_i}]$. The integrals $C_{S,s}^{(1,\dots,6)}$ are as follows:

1. First integral (with $\tilde{q} \equiv q/T$):

$$C_{S,s}^{(1)} = \frac{3T}{2^6 \pi^3 \mathcal{E}_N y_N} \frac{h_t^2 M_i \tilde{m}_i}{v^2} \int_{y_N}^{\infty} d\mathcal{E}_l \int_0^{\mathcal{E}_l + \mathcal{E}_N} d\mathcal{E}_t \Lambda_s^{(N)} I_s^{(1)}, \quad (\text{A.3})$$

$$\begin{aligned} I_s^{(1)} &= \int_{\mathcal{E}_l - y_N}^{\mathcal{E}_l + y_N} d\tilde{q} \frac{(\mathcal{E}_N + \mathcal{E}_l)^2 - z_i^2 - \tilde{q}^2}{(\mathcal{E}_N + \mathcal{E}_l)^2 - \tilde{q}^2} \\ &= \frac{4 y_N (\mathcal{E}_l + \mathcal{E}_N) + z_i^2 \log \left[\frac{(\mathcal{E}_N - y_N)(2\mathcal{E}_l + \mathcal{E}_N - y_N)}{(\mathcal{E}_N + y_N)(2\mathcal{E}_l + \mathcal{E}_N + y_N)} \right]}{2 (\mathcal{E}_l + \mathcal{E}_N)}. \end{aligned} \quad (\text{A.4})$$

2. Second integral:

$$C_{S,s}^{(2)} = \frac{3T}{2^6 \pi^3 \mathcal{E}_N y_N} \frac{h_t^2 M_i \tilde{m}_i}{v^2} \int_0^{y_N} d\mathcal{E}_l \int_0^{\mathcal{E}_l + \mathcal{E}_N} d\mathcal{E}_t \Lambda_s^{(N)} I_s^{(2)}, \quad (\text{A.5})$$

$$\begin{aligned} I_s^{(2)} &= \int_{y_N - \mathcal{E}_l}^{\mathcal{E}_l + y_N} d\tilde{q} \frac{(\mathcal{E}_N + \mathcal{E}_l)^2 - z_i^2 - \tilde{q}^2}{(\mathcal{E}_N + \mathcal{E}_l)^2 - \tilde{q}^2} \\ &= \frac{4 \mathcal{E}_l (\mathcal{E}_l + \mathcal{E}_N) + z_i^2 \log \left[\frac{\mathcal{E}_N^2 - y_N^2}{(2\mathcal{E}_l + \mathcal{E}_N)^2 - y_N^2} \right]}{2 (\mathcal{E}_l + \mathcal{E}_N)}. \end{aligned} \quad (\text{A.6})$$

3. Third integral:

$$C_{S,s}^{(3)} = \frac{3T}{2^6 \pi^3 \mathcal{E}_N y_N} \frac{h_t^2 M_i \tilde{m}_i}{v^2} \int_{y_N}^{\infty} d\mathcal{E}_l \int_0^{\frac{1}{2}(\mathcal{E}_N + y_N)} d\mathcal{E}_t \Lambda_s^{(N)} I_s^{(3)}, \quad (\text{A.7})$$

$$\begin{aligned} I_s^{(3)} &= - \int_{\mathcal{E}_l - y_N}^{\mathcal{E}_l + \mathcal{E}_N - 2\mathcal{E}_t} d\tilde{q} \frac{(\mathcal{E}_N + \mathcal{E}_l)^2 - z_i^2 - \tilde{q}^2}{(\mathcal{E}_N + \mathcal{E}_l)^2 - \tilde{q}^2} \\ &= - \frac{2(\mathcal{E}_l + \mathcal{E}_N)(\mathcal{E}_N - 2\mathcal{E}_t + y_N) + z_i^2 \log \left[\frac{\mathcal{E}_t(2\mathcal{E}_l + \mathcal{E}_N - y_N)}{(\mathcal{E}_l + \mathcal{E}_N - \mathcal{E}_t)(\mathcal{E}_N + y_N)} \right]}{2(\mathcal{E}_l + \mathcal{E}_N)}. \end{aligned} \quad (\text{A.8})$$

4. Fourth integral:

$$C_{S,s}^{(4)} = \frac{3T}{2^6 \pi^3 \mathcal{E}_N y_N} \frac{h_t^2 M_i \tilde{m}_i}{v^2} \int_{y_N}^{\infty} d\mathcal{E}_l \int_{\frac{1}{2}(2\mathcal{E}_l + \mathcal{E}_N - y_N)}^{\mathcal{E}_l + \mathcal{E}_N} d\mathcal{E}_t \Lambda_s^{(N)} I_s^{(4)}, \quad (\text{A.9})$$

$$\begin{aligned} I_s^{(4)} &= - \int_{\mathcal{E}_l - y_N}^{2\mathcal{E}_t - \mathcal{E}_l - \mathcal{E}_N} d\tilde{q} \frac{(\mathcal{E}_N + \mathcal{E}_l)^2 - z_i^2 - \tilde{q}^2}{(\mathcal{E}_N + \mathcal{E}_l)^2 - \tilde{q}^2} \\ &= \frac{2(\mathcal{E}_l + \mathcal{E}_N)(2\mathcal{E}_l + \mathcal{E}_N - 2\mathcal{E}_t - y_N) - z_i^2 \log \left[\frac{(\mathcal{E}_l + \mathcal{E}_N - \mathcal{E}_t)(2\mathcal{E}_l + \mathcal{E}_N - y_N)}{\mathcal{E}_t(\mathcal{E}_N + y_N)} \right]}{2(\mathcal{E}_l + \mathcal{E}_N)}. \end{aligned} \quad (\text{A.10})$$

5. Fifth integral:

$$C_{S,s}^{(5)} = \frac{3T}{2^6 \pi^3 \mathcal{E}_N y_N} \frac{h_t^2 M_i \tilde{m}_i}{v^2} \int_0^{y_N} d\mathcal{E}_l \int_0^{\frac{1}{2}(2\mathcal{E}_l + \mathcal{E}_N - y_N)} d\mathcal{E}_t \Lambda_s^{(N)} I_s^{(5)}, \quad (\text{A.11})$$

$$\begin{aligned} I_s^{(5)} &= - \int_{y_N - \mathcal{E}_l}^{\mathcal{E}_l + \mathcal{E}_N - 2\mathcal{E}_t} d\tilde{q} \frac{(\mathcal{E}_N + \mathcal{E}_l)^2 - z_i^2 - \tilde{q}^2}{(\mathcal{E}_N + \mathcal{E}_l)^2 - \tilde{q}^2} \\ &= - \frac{2(\mathcal{E}_l + \mathcal{E}_N)(2\mathcal{E}_l + \mathcal{E}_N - 2\mathcal{E}_t - y_N) - z_i^2 \log \left[\frac{(\mathcal{E}_l + \mathcal{E}_N - \mathcal{E}_t)(2\mathcal{E}_l + \mathcal{E}_N - y_N)}{\mathcal{E}_t(\mathcal{E}_N + y_N)} \right]}{2(\mathcal{E}_l + \mathcal{E}_N)}. \end{aligned} \quad (\text{A.12})$$

6. Sixth integral:

$$C_{S,s}^{(6)} = \frac{3T}{2^6 \pi^3 \mathcal{E}_N y_N} \frac{h_t^2 M_i \tilde{m}_i}{v^2} \int_0^{y_N} d\mathcal{E}_l \int_{\frac{1}{2}(\mathcal{E}_N + y_N)}^{\mathcal{E}_l + \mathcal{E}_N} d\mathcal{E}_t \Lambda_s^{(N)} I_s^{(6)}, \quad (\text{A.13})$$

$$\begin{aligned} I_s^{(6)} &= - \int_{y_N - \mathcal{E}_l}^{2\mathcal{E}_t - \mathcal{E}_l - \mathcal{E}_N} d\tilde{q} \frac{(\mathcal{E}_N + \mathcal{E}_l)^2 - z_i^2 - \tilde{q}^2}{(\mathcal{E}_N + \mathcal{E}_l)^2 - \tilde{q}^2} \\ &= \frac{2(\mathcal{E}_l + \mathcal{E}_N)(\mathcal{E}_N - 2\mathcal{E}_t + y_N) - z_i^2 \log \left[\frac{(\mathcal{E}_l + \mathcal{E}_N - \mathcal{E}_t)(\mathcal{E}_N + y_N)}{\mathcal{E}_t(2\mathcal{E}_l + \mathcal{E}_N - y_N)} \right]}{2(\mathcal{E}_l + \mathcal{E}_N)}. \end{aligned} \quad (\text{A.14})$$

Lepton asymmetry

For the lepton asymmetry the s -channel phase space element is given by

$$\Lambda_s^{(l-\bar{l})\alpha} \left(f_{(l-\bar{l})\alpha}, f_{N_i}, f_t, t_q \right) = - f_{(l-\bar{l})\alpha} \frac{e^{\mathcal{E}_t} (1 + (e^{\mathcal{E}_l + \mathcal{E}_N} - 1) f_{N_i})}{(1 + e^{\mathcal{E}_t}) (e^{\mathcal{E}_l + \mathcal{E}_N} + e^{\mathcal{E}_t})}, \quad (\text{A.15})$$

and the s -channel contribution to Eq. (3.7) can be expressed as

$$C_{S,s}[f_{(l-\bar{l})\alpha}] = C_{S,s}^{(1)} + C_{S,s}^{(2)} + C_{S,s}^{(3)} + C_{S,s}^{(4)} + C_{S,s}^{(5)} + C_{S,s}^{(6)} \quad (\text{A.16})$$

to be integrated numerically over two remaining degrees of freedom. The explicit integrals in Eq. (A.16) are:

1. First integral

$$C_{S,s}^{(1)} = \frac{3T}{2^6 \pi^3 \mathcal{E}_l^2} \frac{h_t^2 M_i \tilde{m}_i}{v^2} \int_z^{\sqrt{\mathcal{E}_l^2 + z_i^2}} d\mathcal{E}_N \int_0^{\mathcal{E}_l + \mathcal{E}_N} d\mathcal{E}_t \Lambda_s^{(l-\bar{l})} I_s^{(1)}, \quad (\text{A.17})$$

where $I_s^{(1)}$ is given by Eq. (A.4).

2. Second integral with $I_s^{(2)}$ given by Eq. (A.6):

$$C_{S,s}^{(2)} = \frac{3T}{2^6 \pi^3 \mathcal{E}_l^2} \frac{h_t^2 M_i \tilde{m}_i}{v^2} \int_z^\infty d\mathcal{E}_N \int_0^{\mathcal{E}_l + \mathcal{E}_N} d\mathcal{E}_t \Lambda_s^{(l-\bar{l})} I_s^{(2)}. \quad (\text{A.18})$$

3. Third integral ($I_s^{(3)}$ given by Eq. (A.8)):

$$C_{S,s}^{(3)} = \frac{3T}{2^6 \pi^3 \mathcal{E}_l^2} \frac{h_t^2 M_i \tilde{m}_i}{v^2} \int_z^{\sqrt{\mathcal{E}_l^2 + z_i^2}} d\mathcal{E}_N \int_0^{\frac{1}{2}(\mathcal{E}_N + y_N)} d\mathcal{E}_t \Lambda_s^{(l-\bar{l})} I_s^{(3)}. \quad (\text{A.19})$$

4. Fourth integral ($I_s^{(4)}$ given by Eq. (A.10)):

$$C_{S,s}^{(4)} = \frac{3T}{2^6 \pi^3 \mathcal{E}_l^2} \frac{h_t^2 M_i \tilde{m}_i}{v^2} \int_z^{\sqrt{\mathcal{E}_l^2 + z_i^2}} d\mathcal{E}_N \int_{\frac{1}{2}(2\mathcal{E}_l + \mathcal{E}_N - y_N)}^{\mathcal{E}_l + \mathcal{E}_N} d\mathcal{E}_t \Lambda_s^{(l-\bar{l})} I_s^{(4)}. \quad (\text{A.20})$$

5. Fifth integral ($I_s^{(5)}$ given by Eq. (A.12)):

$$C_{S,s}^{(5)} = \frac{3T}{2^6 \pi^3 \mathcal{E}_l^2} \frac{h_t^2 M_i \tilde{m}_i}{v^2} \int_z^\infty d\mathcal{E}_N \int_0^{\frac{1}{2}(2\mathcal{E}_l + \mathcal{E}_N - y_N)} d\mathcal{E}_t \Lambda_s^{(l-\bar{l})} I_s^{(5)}. \quad (\text{A.21})$$

6. Sixth integral ($I_s^{(6)}$ given by Eq. (A.14)):

$$C_{S,s}^{(6)} = \frac{3T}{2^6 \pi^3 \mathcal{E}_l^2} \frac{h_t^2 M_i \tilde{m}_i}{v^2} \int_z^\infty d\mathcal{E}_N \int_{\frac{1}{2}(\mathcal{E}_N + y_N)}^{\mathcal{E}_l + \mathcal{E}_N} d\mathcal{E}_t \Lambda_s^{(l-\bar{l})} I_s^{(6)}. \quad (\text{A.22})$$

B. t -channel collision integrals

Right-handed neutrino

The t -channel phase space element for right-handed neutrinos is given by:

$$\Lambda_t^{(N_i)}(f_{N_i}, f_q, f_{l_\alpha}, f_t) = -\frac{e^{\mathcal{E}_l + \mathcal{E}_q} (-1 + f_{N_i} + e^{\mathcal{E}_N} f_{N_i})}{(1 + e^{\mathcal{E}_l}) (1 + e^{\mathcal{E}_q}) (e^{\mathcal{E}_l} + e^{\mathcal{E}_l + \mathcal{E}_q})}, \quad (\text{B.1})$$

and the t -channel contribution of Eq. (3.5) can equivalently be written as

$$C_{S,t}[f_{N_i}] = C_{S,t}^{(1)} + C_{S,t}^{(2)} + C_{S,t}^{(3)} + C_{S,t}^{(4)}, \quad (\text{B.2})$$

where the constituent integrals are as follows:

1. First integral (with $\tilde{k} \equiv k/T$):

$$\begin{aligned} C_{S,t}^{(1)} &= \frac{3T}{2^6 \pi^3 \mathcal{E}_N y_N} \frac{h_t^2 M_i \tilde{m}_i}{v^2} \int_{\frac{1}{2}(\mathcal{E}_N + y_N)}^{\frac{1}{2}(\mathcal{E}_N + y_N)} d\mathcal{E}_l \int_{\frac{1}{2}(\mathcal{E}_N - y_N + a_h z_i)}^{\frac{1}{2}(2\mathcal{E}_l - \mathcal{E}_N + y_N)} d\mathcal{E}_q \Lambda_t^{(N)} I_t^{(1)}, \quad (\text{B.3}) \\ I_t^{(1)} &= \int_{\mathcal{E}_N - \mathcal{E}_l + a_h z_i}^{2\mathcal{E}_q + \mathcal{E}_N - \mathcal{E}_l} d\tilde{k} \frac{(\mathcal{E}_N - \mathcal{E}_l)^2 - z_i^2 - \tilde{k}^2}{(\mathcal{E}_N - \mathcal{E}_l)^2 - \tilde{k}^2} \\ &= \frac{2(\mathcal{E}_N - \mathcal{E}_l)(2\mathcal{E}_q - a_h z_i) - z_i^2 \log \left[\frac{(\mathcal{E}_N + \mathcal{E}_q - \mathcal{E}_l) a_h z_i}{\mathcal{E}_q (2(\mathcal{E}_N - \mathcal{E}_l) + a_h z_i)} \right]}{2(\mathcal{E}_N - \mathcal{E}_l)}. \end{aligned}$$

2. Second integral:

$$\begin{aligned} C_{S,t}^{(2)} &= \frac{3T}{2^6 \pi^3 \mathcal{E}_N y_N} \frac{h_t^2 M_i \tilde{m}_i}{v^2} \int_{\frac{1}{2}(\mathcal{E}_N + y_N)}^{\frac{1}{2}(\mathcal{E}_N + y_N)} d\mathcal{E}_l \int_{\frac{1}{2}(2\mathcal{E}_l - \mathcal{E}_N + y_N)}^{\infty} d\mathcal{E}_q \Lambda_t^{(N)} I_t^{(2)}, \quad (\text{B.4}) \\ I_t^{(2)} &= \int_{\mathcal{E}_N - \mathcal{E}_l + a_h z_i}^{\mathcal{E}_l + y_N} d\tilde{k} \frac{(\mathcal{E}_N - \mathcal{E}_l)^2 - z_i^2 - \tilde{k}^2}{(\mathcal{E}_N - \mathcal{E}_l)^2 - \tilde{k}^2} \\ &= \frac{2(\mathcal{E}_N - \mathcal{E}_l)(2\mathcal{E}_l - \mathcal{E}_N + y_N - a_h z_i) - z_i^2 \left(\log \left[\frac{-a_h z_i (\mathcal{E}_N + y_N)}{(\mathcal{E}_N - 2\mathcal{E}_l - y_N)(2(\mathcal{E}_N - \mathcal{E}_l) + a_h z_i)} \right] \right)}{2(\mathcal{E}_N - \mathcal{E}_l)}. \end{aligned}$$

3. Third integral:

$$\begin{aligned} C_{S,t}^{(3)} &= \frac{3T}{2^6 \pi^3 \mathcal{E}_N y_N} \frac{h_t^2 M_i \tilde{m}_i}{v^2} \int_{\frac{1}{2}(\mathcal{E}_N + y_N)}^{\infty} d\mathcal{E}_l \int_{\frac{1}{2}(2\mathcal{E}_l - \mathcal{E}_N - y_N)}^{\frac{1}{2}(2\mathcal{E}_l - \mathcal{E}_N + y_N)} d\mathcal{E}_q \Lambda_t^{(N)} I_t^{(3)}, \quad (\text{B.5}) \\ I_t^{(3)} &= \int_{\mathcal{E}_l - y_N}^{2\mathcal{E}_q + \mathcal{E}_N - \mathcal{E}_l} d\tilde{k} \frac{(\mathcal{E}_N - \mathcal{E}_l)^2 - z_i^2 - \tilde{k}^2}{(\mathcal{E}_N - \mathcal{E}_l)^2 - \tilde{k}^2} \\ &= \frac{2(\mathcal{E}_N - \mathcal{E}_l)(\mathcal{E}_N + y_N + 2(\mathcal{E}_q - \mathcal{E}_l)) + z_i^2 \left(\log \left[-\frac{-\mathcal{E}_q (\mathcal{E}_N - y_N)}{(\mathcal{E}_N + \mathcal{E}_q - \mathcal{E}_l)(\mathcal{E}_N - 2\mathcal{E}_l + y_N)} \right] \right)}{2(\mathcal{E}_N - \mathcal{E}_l)}. \end{aligned}$$

4. Fourth integral:

$$\begin{aligned}
C_{S,t}^{(4)} &= \frac{3T}{2^6 \pi^3 \mathcal{E}_N y_N} \frac{h_t^2 M_i \tilde{m}_i}{v^2} \int_{\frac{1}{2}(\mathcal{E}_N + y_N)}^{\infty} d\mathcal{E}_l \int_{\frac{1}{2}(\mathcal{E}_l - \mathcal{E}_N + y_N)}^{\infty} d\mathcal{E}_q \Lambda_t^{(N)} I_t^{(4)}, \quad (\text{B.6}) \\
I_t^{(4)} &= \int_{\mathcal{E}_l - y_N}^{\mathcal{E}_l + y_N} d\tilde{k} \frac{(\mathcal{E}_N - \mathcal{E}_l)^2 - z_i^2 - \tilde{k}^2}{(\mathcal{E}_N - \mathcal{E}_l)^2 - \tilde{k}^2} \\
&= \frac{4(\mathcal{E}_N - \mathcal{E}_l) y_N + z_i^2 \log \left[\frac{(\mathcal{E}_N - y_N)(\mathcal{E}_N - y_N - 2\mathcal{E}_l)}{(\mathcal{E}_N + y_N)(\mathcal{E}_N + y_N - 2\mathcal{E}_l)} \right]}{2(\mathcal{E}_N - \mathcal{E}_l)}.
\end{aligned}$$

In the integrals (B.3) and (B.4) we have introduced $a_h = m_\Phi/M_i$ as an infrared cut-off for the t -channel diagram, where m_Φ is the mass of the Higgs boson which presumably receives contributions from interactions with the thermal bath, i.e., its value does not correspond to that potentially measured at the LHC. The value of m_Φ can in principle be deduced from a thermal field theoretic treatment of leptogenesis, and the analysis of [28] found $m_\Phi(T) \simeq 0.4T$. However some open questions still remain and hence in the present work we prefer to adopt a value of $a_h = 10^{-5}$, used first by Luty in [57].

Lepton asymmetry

The t -channel phase space element for the lepton asymmetry is given as

$$\Lambda_t^{(l-\bar{l})\alpha} \left(f_{(l-\bar{l})\alpha}, f_t, f_{N_i}, f_q \right) = f_{(l-\bar{l})\alpha} \frac{e^{\mathcal{E}_q} (e^{\mathcal{E}_l} (-1 + f_{N_i}) - e^{\mathcal{E}_N} f_{N_i})}{(1 + e^{\mathcal{E}_q}) (e^{\mathcal{E}_N} + e^{\mathcal{E}_q + \mathcal{E}_l})}. \quad (\text{B.7})$$

As in Section B we cut-off the integrand in $C_{S,t}^{(1)}$ and $C_{S,t}^{(2)}$ by adding a_h in the lower integration limit of k (modifying the limits of \mathcal{E}_q and \mathcal{E}_N accordingly).

The t -channel contribution of the collision integral (3.7) can then equivalently be written as

$$C_{S,t}[f_{(l-\bar{l})\alpha}] = C_{S,t}^{(1)} + C_{S,t}^{(2)} + C_{S,t}^{(3)} + C_{S,t}^{(4)}, \quad (\text{B.8})$$

with:

1. First integral:

$$\begin{aligned}
C_{S,t}^{(1)} &= \frac{3T}{2^6 \pi^3 \mathcal{E}_N y_N} \frac{h_t^2 M_i \tilde{m}_i}{v^2} \int_{\frac{(2\mathcal{E}_l - a_h z_i)^2 + z_i^2}{2(2\mathcal{E}_l - a_h z_i)}}^{\infty} d\mathcal{E}_N \int_{\mathcal{E}_N - \mathcal{E}_l + \frac{1}{2}a_h z_i}^{\frac{1}{2}(\mathcal{E}_N + y_N)} d\mathcal{E}_q \Lambda_t^{(l-\bar{l})} I_t^{(1)}, \quad (\text{B.9}) \\
I_t^{(1)} &= \int_{\mathcal{E}_N - \mathcal{E}_l + a_h z_i}^{2\mathcal{E}_q + \mathcal{E}_l - \mathcal{E}_N} d\tilde{k} \frac{(\mathcal{E}_N - \mathcal{E}_l)^2 - z_i^2 - \tilde{k}^2}{(\mathcal{E}_N - \mathcal{E}_l)^2 - \tilde{k}^2} \\
&= - \frac{2(\mathcal{E}_N - \mathcal{E}_l) (2(\mathcal{E}_N - \mathcal{E}_q - \mathcal{E}_l) + a_h z_i) + z_i^2 \log \left[\frac{\mathcal{E}_q a_h z_i}{(\mathcal{E}_q - \mathcal{E}_N + \mathcal{E}_l)(2(\mathcal{E}_N - \mathcal{E}_l) + a_h z_i)} \right]}{2(\mathcal{E}_N - \mathcal{E}_l)}.
\end{aligned}$$

2. Second integral:

$$C_{S,t}^{(2)} = \frac{3T}{2^6 \pi^3 \mathcal{E}_N y_N} \frac{h_t^2 M_i \tilde{m}_i}{v^2} \int_{\frac{(2\mathcal{E}_l - a_h z_i)^2 + z_i^2}{2(2\mathcal{E}_l - a_h z_i)}}^{\infty} d\mathcal{E}_N \int_{\frac{1}{2}(\mathcal{E}_N + y_N)}^{\infty} d\mathcal{E}_q \Lambda_t^{(l-\bar{l})} I_t^{(2)}, \quad (\text{B.10})$$

$$I_t^{(2)} = \int_{\mathcal{E}_N - \mathcal{E}_l + a_h z_i}^{\mathcal{E}_l + y_N} d\tilde{k} \frac{(\mathcal{E}_N - \mathcal{E}_l)^2 - z_i^2 - \tilde{k}^2}{(\mathcal{E}_N - \mathcal{E}_l)^2 - \tilde{k}^2}$$

$$= \frac{2(\mathcal{E}_N - \mathcal{E}_l)(2\mathcal{E}_l - \mathcal{E}_N + y_N - a_h z_i) - z_i^2 \log \left[\frac{(\mathcal{E}_N + y_N) a_h z_i}{(2\mathcal{E}_l - \mathcal{E}_N + y_N)(2(\mathcal{E}_N - \mathcal{E}_l) + a_h z_i)} \right]}{2(\mathcal{E}_N - \mathcal{E}_l)}.$$

3. Third integral:

$$C_{S,t}^{(3)} = \frac{3T}{2^6 \pi^3 \mathcal{E}_N y_N} \frac{h_t^2 M_i \tilde{m}_i}{v^2} \int_{z_i}^{\frac{4\mathcal{E}_l^2 + z_i^2}{4\mathcal{E}_l}} d\mathcal{E}_N \int_{\frac{1}{2}(\mathcal{E}_N - y_N)}^{\frac{1}{2}(\mathcal{E}_N + y_N)} d\mathcal{E}_q \Lambda_t^{(l-\bar{l})} I_t^{(3)}, \quad (\text{B.11})$$

$$I_t^{(3)} = \int_{\mathcal{E}_l - y_N}^{2\mathcal{E}_q + \mathcal{E}_l - \mathcal{E}_N} d\tilde{k} \frac{(\mathcal{E}_N - \mathcal{E}_l)^2 - z_i^2 - \tilde{k}^2}{(\mathcal{E}_N - \mathcal{E}_l)^2 - \tilde{k}^2}$$

$$= \frac{2(\mathcal{E}_N - \mathcal{E}_l)(2\mathcal{E}_q - \mathcal{E}_N + y_N) + z_i^2 \log \left[\frac{(\mathcal{E}_N - \mathcal{E}_q - \mathcal{E}_l)(\mathcal{E}_N - y_N)}{\mathcal{E}_q(\mathcal{E}_N - 2\mathcal{E}_l + y_N)} \right]}{2(\mathcal{E}_N - \mathcal{E}_l)}.$$

4. Fourth integral:

$$C_{S,t}^{(4)} = \frac{3T}{2^6 \pi^3 \mathcal{E}_N y_N} \frac{h_t^2 M_i \tilde{m}_i}{v^2} \int_{z_i}^{\frac{4\mathcal{E}_l^2 + z_i^2}{4\mathcal{E}_l}} d\mathcal{E}_N \int_{\frac{1}{2}(\mathcal{E}_N + y_N)}^{\infty} d\mathcal{E}_q \Lambda_t^{(l-\bar{l})} I_t^{(4)}, \quad (\text{B.12})$$

$$I_t^{(4)} = \int_{\mathcal{E}_l - y_N}^{\mathcal{E}_l + y_N} d\tilde{k} \frac{(\mathcal{E}_N - \mathcal{E}_l)^2 - z_i^2 - \tilde{k}^2}{(\mathcal{E}_N - \mathcal{E}_l)^2 - \tilde{k}^2}$$

$$= \frac{4(\mathcal{E}_N - \mathcal{E}_l)y_N + z_i^2 \log \left[\frac{(\mathcal{E}_N - 2\mathcal{E}_l - y_N)(\mathcal{E}_N - y_N)}{(\mathcal{E}_N - 2\mathcal{E}_l + y_N)(\mathcal{E}_N + y_N)} \right]}{2(\mathcal{E}_N - \mathcal{E}_l)}.$$

C. Reaction rates in the integrated picture

The decay interaction term D_i in the Boltzmann equations (3.9) and (3.10) is given by

$$D_i \equiv z_i K_i \left\langle \frac{M_i}{E_N} \right\rangle. \quad (\text{C.1})$$

The scattering rate S_i consists of two terms, $S_i = 2S_s + 4S_t$, coming respectively from scattering in the s -channel and in the t -channel. One factor of 2 stems from contributions from processes involving anti-particles, and another factor of 2 in the t -channel term originates from the u -channel diagram.

It is convenient to rewrite the s - and t -channel scattering rates $S_{(s,t)_i}$ in terms of the functions $f_{(s,t)_i}$, defined as

$$f_{(s,t)_i}(z_i) = \frac{\int_{z_i^2}^{\infty} d\Psi \chi_{s,t}(\Psi/z_i^2) \sqrt{\Psi} K_1(\sqrt{\Psi})}{z_i^2 K_2(z_i)}, \quad (\text{C.2})$$

such that

$$S_{(s,t)_i} = \frac{K_{S_i}}{9\zeta(3)} f_{(s,t)_i}, \quad (\text{C.3})$$

and the total scattering rate is given by

$$S_i = \frac{2K_{S_i}}{9\zeta(3)} (f_{s_i}(z_i) + 2f_{t_i}(z_i)), \quad (\text{C.4})$$

where

$$K_{S_i} = \frac{\tilde{m}_i}{m_*^S}, \quad m_*^S = \frac{4\pi^2}{9} \frac{g_N}{h_t^2(T)} m_*, \quad (\text{C.5})$$

with \tilde{m}_i and m_* defined in Eqs. (1.11).

The functions $\chi_{s,t}(x)$ are defined as

$$\chi_s(x) = \left(\frac{x-1}{x} \right)^2, \quad (\text{C.6})$$

$$\chi_t(x) = \frac{x-1}{x} \left[\frac{x-2+2a_h}{x-1+a_h} + \frac{1-2a_h}{x-1} \log \left(\frac{x-1+a_h}{a_h} \right) \right], \quad (\text{C.7})$$

where again $a_h = m_\Phi/M_i$ is the infrared cut-off for the t -channel diagram.

The total wash-out rate is given by

$$W_i = W_{ID_i} \left[1 + \frac{1}{D_i} \left(2 \frac{N_{N_i}}{N_{N_i}^{\text{eq}}} S_{s_i} + 4 S_{t_i} \right) \right] \quad (\text{C.8})$$

where W_{ID_i} quantifies the strength of the wash-out due to inverse decays

$$W_{ID_i} \equiv \frac{1}{2} D_i \frac{N_{N_i}^{\text{eq}}}{N_l^{\text{eq}}}, \quad (\text{C.9})$$

and the equilibrium abundances are $N_l^{\text{eq}} = 3/4$, and $N_{N_i}^{\text{eq}}(z) = \frac{3}{8} z_i^2 K_2(z_i)$.

References

- [1] P. Minkowski, *mu* → *e* gamma at a rate of one out of 1-billion muon decays?, *Phys. Lett.* **B67** (1977) 421.
- [2] T. Yanagida, *Proceedings of the Workshop on Unified Theories and Baryon Number in the Universe*. KEK report 79-18, 1979. p.95.
- [3] M. Gell-Man, P. Ramond, and R. Slansky, *Supergravity*. North Holland, Amsterdam, 1979. eds. P.van Nieuwenhuizen, D.Freedman, p.315.
- [4] R. Barbieri, D. V. Nanopoulos, G. Morchio, and F. Strocchi, *Neutrino Masses in Grand Unified Theories*, *Phys. Lett.* **B90** (1980) 91.
- [5] R. N. Mohapatra and G. Senjanovic, *Neutrino Masses and Mixings in Gauge Models with Spontaneous Parity Violation*, *Phys. Rev.* **D23** (1981) 165.

- [6] M. Fukugita and T. Yanagida, *Baryogenesis without grand unification*, *Phys. Lett.* **B174** (1986) 45.
- [7] F. R. Klinkhamer and N. S. Manton, *A saddle point solution in the weinberg-salam theory*, *Phys. Rev.* **D30** (1984) 2212.
- [8] A. Abada, S. Davidson, F.-X. Josse-Michaux, M. Losada, and A. Riotto, *Flavour Issues in Leptogenesis*, *JCAP* **0604** (2006) 004, [hep-ph/0601083].
- [9] A. Abada *et. al.*, *Flavour matters in leptogenesis*, *JHEP* **09** (2006) 010, [hep-ph/0605281].
- [10] E. Nardi, Y. Nir, E. Roulet, and J. Racker, *The importance of flavor in leptogenesis*, *JHEP* **01** (2006) 164, [hep-ph/0601084].
- [11] S. Blanchet and P. Di Bari, *Flavor effects on leptogenesis predictions*, *JCAP* **0703** (2007) 018, [hep-ph/0607330].
- [12] S. Blanchet, P. Di Bari, and G. G. Raffelt, *Quantum Zeno effect and the impact of flavor in leptogenesis*, *JCAP* **0703** (2007) 012, [hep-ph/0611337].
- [13] M. Flanz, E. A. Paschos, and U. Sarkar, *Baryogenesis from a lepton asymmetric universe*, *Phys. Lett.* **B345** (1995) 248–252, [hep-ph/9411366].
- [14] L. Covi, E. Roulet, and F. Vissani, *CP violating decays in leptogenesis scenarios*, *Phys. Lett.* **B384** (1996) 169–174, [hep-ph/9605319].
- [15] W. Buchmüller and M. Plümacher, *Neutrino masses and the baryon asymmetry*, *Int. J. Mod. Phys.* **A15** (2000) 5047–5086, [hep-ph/0007176].
- [16] M. Plümacher, *Baryogenesis and lepton number violation*, *Z. Phys.* **C74** (1997) 549–559, [hep-ph/9604229].
- [17] W. Buchmüller, P. Di Bari, and M. Plümacher, *Leptogenesis for pedestrians*, *Ann. Phys.* **315** (2005) 305–351, [hep-ph/0401240].
- [18] M. Plümacher, *Baryon asymmetry, neutrino mixing and supersymmetric SO(10) unification*, *Nucl. Phys.* **B530** (1998) 207–246, [hep-ph/9704231].
- [19] W. Buchmüller and M. Plümacher, *Baryon asymmetry and neutrino mixing*, *Phys. Lett.* **B389** (1996) 73–77, [hep-ph/9608308].
- [20] P. H. Chankowski and K. Turzyski, *Limits on $T(\text{reh})$ for thermal leptogenesis with hierarchical neutrino masses*, *Phys. Lett.* **B570** (2003) 198–204, [arXiv:hep-ph/0306059].
- [21] P. Di Bari, *Seesaw geometry and leptogenesis*, *Nucl. Phys.* **B727** (2005) 318–354, [hep-ph/0502082].
- [22] F. Hahn-Woernle, M. Plümacher, and Y. Y. Y. Wong, *Full Boltzmann equations for leptogenesis including scattering*, *JCAP* **0908** (2009) 028, [arXiv:0907.0205].
- [23] J. Garayoa, S. Pastor, T. Pinto, N. Rius, and O. Vives, *On the full Boltzmann equations for Leptogenesis*, arXiv:0905.4834.
- [24] K. S. Babu, C. N. Leung, and J. T. Pantaleone, *Renormalization of the neutrino mass operator*, *Phys. Lett.* **B319** (1993) 191–198, [hep-ph/9309223].
- [25] S. Antusch, J. Kersten, M. Lindner, and M. Ratz, *Running neutrino masses, mixings and CP phases: Analytical results and phenomenological consequences*, *Nucl. Phys.* **B674** (2003) 401–433, [hep-ph/0305273].

- [26] J. A. Casas and A. Ibarra, *Oscillating neutrinos and $\mu \rightarrow e, \gamma$* , *Nucl. Phys.* **B618** (2001) 171–204, [hep-ph/0103065].
- [27] S. Blanchet and P. Di Bari, *Leptogenesis beyond the limit of hierarchical heavy neutrino masses*, *JCAP* **0606** (2006) 023, [hep-ph/0603107].
- [28] G. F. Giudice, A. Notari, M. Raidal, A. Riotto, and A. Strumia, *Towards a complete theory of thermal leptogenesis in the sm and mssm*, *Nucl. Phys.* **B685** (2004) 89–149, [hep-ph/0310123].
- [29] F. Hahn-Woernle and M. Plümacher, *Effects of reheating on leptogenesis*, *Nucl. Phys.* **B806** (2009) 68–83, [arXiv:0801.3972].
- [30] S. Davidson and A. Ibarra, *A lower bound on the right-handed neutrino mass from leptogenesis*, *Phys. Lett.* **B535** (2002) 25–32, [hep-ph/0202239].
- [31] W. Buchmüller, P. Di Bari, and M. Plümacher, *The neutrino mass window for baryogenesis*, *Nucl. Phys.* **B665** (2003) 445–468, [hep-ph/0302092].
- [32] T. Moroi, H. Murayama, and M. Yamaguchi, *Cosmological constraints on the light stable gravitino*, *Phys. Lett.* **B303** (1993) 289–294.
- [33] M. Bolz, A. Brandenburg, and W. Buchmüller, *Thermal production of gravitinos*, *Nucl. Phys.* **B606** (2001) 518–544, [hep-ph/0012052].
- [34] M. Kawasaki, K. Kohri, and T. Moroi, *Big-bang nucleosynthesis and hadronic decay of long-lived massive particles*, *Phys. Rev.* **D71** (2005) 083502, [astro-ph/0408426].
- [35] J. Pradler and F. D. Steffen, *Thermal Gravitino Production and Collider Tests of Leptogenesis*, *Phys. Rev.* **D75** (2007) 023509, [hep-ph/0608344].
- [36] S. Davidson, *From weak-scale observables to leptogenesis*, *JHEP* **03** (2003) 037, [hep-ph/0302075].
- [37] G. C. Branco, R. Gonzalez Felipe, F. R. Joaquim, and M. N. Rebelo, *Leptogenesis, CP violation and neutrino data: What can we learn?*, *Nucl. Phys.* **B640** (2002) 202–232, [hep-ph/0202030].
- [38] K. S. Babu, J. C. Pati, and F. Wilczek, *Fermion masses, neutrino oscillations, and proton decay in the light of SuperKamiokande*, *Nucl. Phys.* **B566** (2000) 33–91, [hep-ph/9812538].
- [39] S. F. King and G. G. Ross, *Fermion masses and mixing angles from SU(3) family symmetry*, *Phys. Lett.* **B520** (2001) 243–253, [hep-ph/0108112].
- [40] M. Raidal, A. Strumia, and K. Turzynski, *Low-scale standard supersymmetric leptogenesis*, *Phys. Lett.* **B609** (2005) 351–359, [hep-ph/0408015].
- [41] O. Vives, *Flavoured leptogenesis: A successful thermal leptogenesis with $N(1)$ mass below 10^{10} -GeV*, *Phys. Rev.* **D73** (2006) 073006, [hep-ph/0512160].
- [42] R. Barbieri, P. Creminelli, A. Strumia, and N. Tetradis, *Baryogenesis through leptogenesis*, *Nucl. Phys.* **B575** (2000) 61–77, [hep-ph/9911315].
- [43] A. Strumia, *Baryogenesis via leptogenesis*, hep-ph/0608347.
- [44] G. Engelhard, Y. Grossman, E. Nardi, and Y. Nir, *The importance of N_2 leptogenesis*, *Phys. Rev. Lett.* **99** (2007) 081802, [hep-ph/0612187].
- [45] S. Blanchet, *A New Era of Leptogenesis*, arXiv:0807.1408.
- [46] S. Blanchet and P. Di Bari, *New aspects of leptogenesis bounds*, *Nucl. Phys.* **B807** (2009) 155–187, [arXiv:0807.0743].

- [47] A. Pilaftsis and T. E. J. Underwood, *Resonant leptogenesis*, *Nucl. Phys.* **B692** (2004) 303–345, [hep-ph/0309342].
- [48] A. Pilaftsis and T. E. J. Underwood, *Electroweak-scale resonant leptogenesis*, *Phys. Rev.* **D72** (2005) 113001, [hep-ph/0506107].
- [49] E. Nardi, J. Racker, and E. Roulet, *CP violation in scatterings, three body processes and the Boltzmann equations for leptogenesis*, *JHEP* **09** (2007) 090, [arXiv:0707.0378].
- [50] A. Basbøll and S. Hannestad, *Decay of heavy Majorana neutrinos using the full Boltzmann equation including its implications for leptogenesis*, *JCAP* **0701** (2007) 003, [hep-ph/0609025].
- [51] E. W. Kolb and S. Wolfram, *Baryon Number Generation in the Early Universe*, *Nucl. Phys.* **B172** (1980) 224.
- [52] F. T. Hahn-Woernle, *Full Boltzmann equations for leptogenesis*. Dissertation, Technische Universität München, München, 2009. <http://mediatum2.ub.tum.de/node?id=813029>.
- [53] **WMAP** Collaboration, J. Dunkley *et. al.*, *Five-Year Wilkinson Microwave Anisotropy Probe (WMAP) Observations: Likelihoods and Parameters from the WMAP data*, arXiv:0803.0586.
- [54] W. Buchmüller, P. Di Bari, and M. Plümacher, *Cosmic microwave background, matter-antimatter asymmetry and neutrino masses*, *Nucl. Phys.* **B643** (2002) 367–390, [hep-ph/0205349].
- [55] **Particle Data Group** Collaboration, W. M. Yao *et. al.*, *Review of particle physics*, *J. Phys.* **G33** (2006) 1–1232.
- [56] P. Di Bari and A. Riotto, *Successful type I Leptogenesis with SO(10)-inspired mass relations*, *Phys. Lett.* **B671** (2009) 462–469, [arXiv:0809.2285].
- [57] M. A. Luty, *Baryogenesis via leptogenesis*, *Phys. Rev.* **D45** (1992) 455–465.
- [58] S. Antusch, P. Di Bari, D. A. Jones and S. F. King, *A fuller flavour treatment of N_2 -dominated leptogenesis*, [arXiv:1003.5132].